

# Multi-level Methods for Combined Diagnostics and Prognostics

Gautam Biswas<sup>1</sup> and Sankaran Mahadevan<sup>2</sup>

<sup>1</sup>Department of EECS & ISIS <sup>2</sup>Department of Civil and Environmental Engineering  
Vanderbilt University  
Nashville, TN 37235

[gautam.biswas@vanderbilt.edu](mailto:gautam.biswas@vanderbilt.edu) [sankaran.mahadevan@vanderbilt.edu](mailto:sankaran.mahadevan@vanderbilt.edu)

## Abstract

Integrated Systems Health Management (ISHM) provides the ability to maintain system health and performance over the life of safety-critical systems. This paper discusses a model-based approach to diagnosis and prognosis of safety-critical systems that combines fault detection, isolation and identification, fault-adaptive control, and prognosis into a common framework. At the core of this framework are a set of component oriented physical system models. By incorporating physics of failure models into component models the dynamic behavior of a failing or degrading system can be derived by simulation. Current state information predicts future behavior and performance of the system to guide decision making on system operation and maintenance.

## Introduction

Complex, safety-critical systems, such as aircraft, spacecraft, and power plants have interacting subsystems that operate in multiple physical domains. A number of catastrophic accidents involving these systems have demonstrated that they can degrade and fail in ways that are hard to predict at design time. The need for accurate assessment of system health and performance has generated increased demands for systematic monitoring, analysis, and decision making schemes during system operation. The drive toward increased safety and autonomy imposes requirements for system operation and performance in the presence of degradation and faults in components as well as timely condition-based maintenance to avoid long periods of downtime and catastrophic failures.

Integrated Systems Health Management (ISHM) provides the ability to maintain system health and performance over the life of a system. For safety-critical systems, such as aircraft, ISHM must maintain safe operations while increasing availability by preserving functionality and minimizing downtime. This paper adopts a model-based approach to ISHM that combines fault detection, isolation and identification, fault-adaptive control, prognosis, and maintenance operations into a common framework. At the core of this framework are a set of component-oriented physical system models that define the overall system behavior and performance. By incorporating structural- and material-related physics of failure models into component

models, the behavior of a failing or degrading component can be projected onto system behavior and performance using simulation methods. The overall approach uses current state information, which includes information on the state of the components and system operations data to predict future behavior and performance of the system. Analysis of this information can guide decision making on system operations and condition-based maintenance.

In this paper we focus on model-based approaches to support monitoring, diagnosis, and prognosis tasks for ISHM of multi-domain complex systems. We adopt a multi-level modeling scheme that combines system to subsystem to component-level modeling. System-level models focus on performance parameters, such as the fuel consumed and the thrust generated by an aircraft engine, or the temperature and pressure of superheated steam generated in nuclear power plant. Our hierarchical modeling methodology uses energy conservation and transfer relations to model the interactions between components that make up subsystems, and subsystems that are composed to define the system. The models are parameterized to identify faults and degradations in components that may affect system performance. Component-level models also include structural and material properties to help analyze the root causes of failures and degradations that may occur in components. For example, component model analysis may determine that the decrease in pump (subsystem) efficiency can be attributed to a crack in a rotor vane (component of pump subsystem).

Fig.1 illustrates a layered approach to developing an ISHM computational architecture, with the core infrastructure being supported by model-based approaches for analysis and control at all levels of the system. The figure combines reconfiguration approaches for fault-adaptive control (FAC) [1] and maintenance decisions (a form of reconfiguration) into the supervisory control layer. Model-based Monte Carlo simulation schemes form the basis for designing prognosis algorithms directed toward predicting future system performance and remaining life of components. The derived information is used for a variety of decision-making tasks, such as scheduling, resource allocation and control for system operations, and maintenance and repair tasks to maintain system health and safety. For clarification, we make a distinction between data driven and model driven approaches to prognosis. Data driven approaches re-

ly on historical data patterns and classifier schemes to establish trends and predict future behavior [6]. They are effective only if reliable historical data is available. This is not always the case, therefore, we propose a more general model driven approach to predicting future behavior by *simulating* the changing system model.

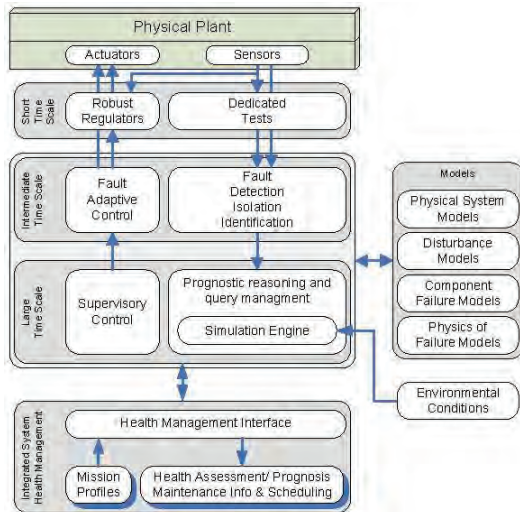


Fig. 1: Computational Architecture of an ISHM system.

We demonstrate our approach on a secondary sodium cooling system of a nuclear reactor. We model the system in the mechanical and fluid domains. To illustrate our multi-level modeling approach, we build a subsystem model of the centrifugal pump that pumps the liquid sodium through the coolant loop from its components. This approach to multi-level modeling easily applies to aircraft systems, such as the fuel transfer system, and the engine cooling and lubrication systems. In other work, we have developed more extensive fluid-thermal models of cooling and lubrication systems [5] for diagnostic analysis.

### Modeling for Diagnosis and Prognosis

Our approach to multi-level modeling of complex systems combines *system*, *subsystem*, and *component-level modeling*. At the *system-level*, modeling generates a description

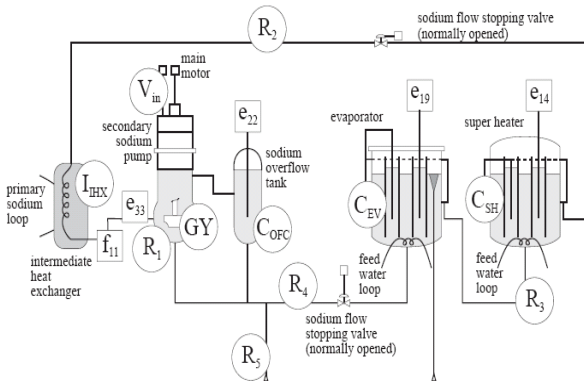


Fig. 2(a): Secondary sodium cooling loop schematic;

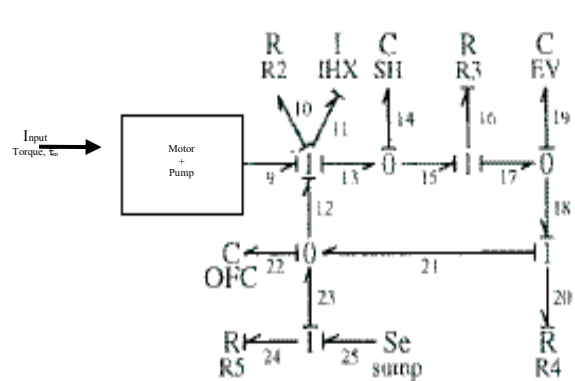
of the system in terms of its constituent *subsystems*, and the subsystem models are a composition of their constituent *components* [11]. The dynamic system behavior is derived using laws of physics (conservation of energy and momentum). For example, consider the schematic of a secondary sodium cooling loop of a nuclear reactor shown in Fig. 2(a). In the nuclear reactor heat from the reactor core is transported to the turbine by a primary and secondary cooling system. The primary cooling subsystem connects directly to the reactor and transfers heat to the secondary cooling subsystem, which then transfers heat carried by the liquid sodium to produce steam in the generator. Heat transfer from the primary cooling loop to the liquid sodium in the secondary loop happens through the intermediate heat exchanger subsystem. The heated sodium is then pumped through two stages: the super heater and the evaporator vessel subsystems both of which provide heat to the steam water loop that drives the turbine subsystem. The system-level hydraulics model is constructed by identifying the subsystem models described above along with connecting pipes and valves.

*Component-level* behaviors are modeled by their structural and material properties. For example, the behavior and performance of the rotor vane component of the pump subsystem is derived as a function of its cross sectional area and its curvature. *Root causes* for degradation of vane behavior, such as corrosion and erosion, can be linked to the rotor parameters. We propose a methodology for modeling structural and material damage mechanisms of components in terms of their material properties, geometry, boundary conditions, and operating conditions. This provides the important link between structural and material *physics of failure* models and the performance-related system models.

### Building System Models: Sodium Cooling Loop

Physics-based modeling of the secondary sodium cooling loop system captures the energy interactions and energy flow between the mechanical, fluid, and thermal components in the system [12]. The subsystem behavior models are composed to derive the system behavior model using a top-down approach.

*Bond graphs* [7] provide an energy-based compositional modeling framework for multi-domain physical system modeling. They represent a domain-independent, topologi-



2(b): Bond Graph Model of Cooling Loop

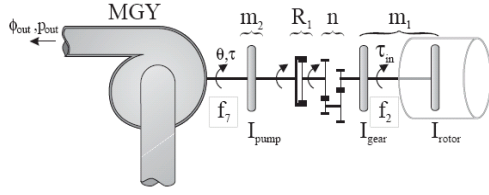


Fig. 3(a): Centrifugal Pump System – Main motor drive + Pump.

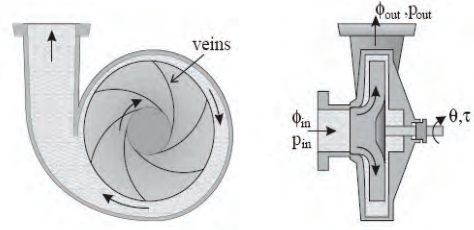


Fig. 3(b): Operation of Centrifugal Pump

cal, lumped-parameter modeling scheme that captures the energy exchange mechanisms in physical processes. The nodes of a bond graph are primitive elements that include energy storage (C and I), energy dissipation (R), energy transformation (TF and GY), and input-output elements (Se and Sf). The connecting edges called *bonds* are energy pathways between the elements. Each bond is associated with two variables: *effort* and *flow*. The product of effort and flow is *power*, i.e., the rate of energy transfer. Connections in the system are modeled by two idealized elements: 0- (or parallel) and 1- (or series) junctions. For a 0- (1-) junction, the efforts (flows) of all incident bonds are equal, and the sum of flows (efforts) is zero. Component parameters of nonlinear models are algebraic functions of other system variables and external input signals, called modulating functions.

The details of the secondary sodium cooling loop model with its subsystems illustrated in Fig. 2(a) are presented next.

**Secondary Cooling Loop Bond Graph Model.** The bond graph model of the secondary sodium cooling loop system captures the energy interactions in the fluid domain and the mechanical interactions between the motor and pump components. The nonlinear, sixth order bond graph model shown in Fig. 2(b). The main motor model (Fig. 3) is simplified to represent a source of mechanical energy with a given torque/angular velocity characteristic. Details of the pump subsystem model are presented later.

The hydraulics of the sodium loop is modeled by a closed power loop (Fig. 2(b)). The coil in the intermediate heat exchanger, represented by a fluid inertia,  $I_{IHx}$ , provides the flow momentum build-up. The piping from the pump through the heat exchanger to the evaporator vessel is represented by resistance  $R_2$ . The two sodium vessels are modeled by capacitances,  $C_{SH}$  and  $C_{EV}$ , and the connecting pipe by its resistance,  $R_3$ . An overflow column,  $C_{OFC}$ , maintains a desired sodium level in the motor, and the piping between the evaporator and this column is represented by resistance,  $R_4$ . This storage facility is connected to a sump,  $Se$ , by a pipe with resistance,  $R_5$ .

### Subsystem model of the Centrifugal Pump

The mechanical and fluid components of the pump are illustrated in Fig.3(a).

**Basic Principles that govern Centrifugal Pump Behavior.** The simplified physical model of a centrifugal pump is derived using conservation of power and momentum. The corresponding equation is  $\tau \cdot \theta = p_{out} \cdot \phi_{out}$ , where  $\tau$  is the input torque,  $\theta$  represents angular velocity of the pump rotor,  $p_{out}$  is the pump pressure, and  $\phi_{out}$  is the corresponding mass flow rate.

By conservation of momentum we get the mechanical momentum  $\int \tau \cdot dt$  equals the hydraulic momentum, which equals the amount of mass moved by the pump times the flowrate. The mass moved depends on the total area of the pump vanes,  $c$  minus the effective loss in moved mass due to the curvature of the vanes,  $b$ . This is computed as  $\int (a \cdot \theta - b \cdot \phi_{out}) dt$ , therefore, the hydraulic momentum of the pump is equal to  $\phi_{out} \int (a \cdot \theta - b \cdot \phi_{out}) dt$ , and

$$\int \tau \cdot dt = \phi_{out} \int (a \cdot \theta - b \cdot \phi_{out}) dt \quad (1)$$

Equation (1) can be rewritten as:

$\tau = \phi_{out}(a \cdot \theta - b \cdot \phi_{out}) + \phi_{out} \int (a \cdot \theta - b \cdot \phi_{out}) dt$ , which for relatively low flow accelerations compared to flow velocity, yields the constituent relation  $\tau = \phi_{out}(a \cdot \theta - b \cdot \phi_{out})$ . From this we derive

$$p_{out} = (a \cdot \theta - b \cdot \phi_{out}) \theta \quad (3)$$

Equation 3 describes a modulated gyrator model with modulus  $(a \cdot \theta - b \cdot \phi_{out})$ .

### Bond graph Model of the Centrifugal Pump subsystem.

The simplified bond graph model of the pump subsystem, shown in Fig. 4, contains the motor system, which converts electrical energy into rotational mechanical energy, the coupling between the motor and pump systems, and the transmission of mechanical to fluid energy by the pump system.

The inertia of the rotor and the mass of transmission gear are modeled by mass parameter,  $m_1$ . The transmission ratio between motor and pump is captured by the transformer

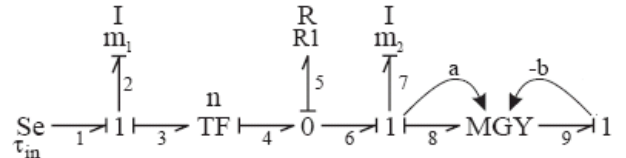


Fig. 4: System-level model of Pump System using a Bond Graph Approach

parameter,  $n$ . Pump losses in the fluid connection between the motor and pump are modeled by a dissipation element,  $R_l$ , and the pump inertia is represented as  $m_2$ . The parameters  $a$  (cross sectional area of veins) and  $b$  (curvature of the veins) of the modulated gyrator, MGY that models the change of mechanical to fluid energy were discussed in the last section. Additional details are provided in [12],[14].

**Component Models: Linking fault parameters to Root Causes using Physics of Failure Models.** Physical damage of many different forms, mechanical and chemical, can affect the performance of centrifugal pump systems (e.g., output pressure and flow rate). This includes structural and material processes, such as corrosion, erosion, wear, and fatigue. By monitoring the change of the system behavior and performance (we discuss our model-based approach to monitoring and FDI in the next section), it is possible to detect and isolate the local damage that is responsible for the pump performance degradation. We develop *physics of failure* (POF) models that link local damage attributed to structural and material changes to subsystem model parameters. Through these parameters, the root cause for damage in components can be linked to subsystem behavior and performance changes, e.g., a change in the surface area of pump vanes due to corrosion increase the losses in the pump.

A more complete methodology would require complex finite element models to compute degradation effects on component behavior. Instead, we develop simpler mathematical models to represent POF phenomena. An example POF model is used to illustrate our integrated modeling methodology. The physics of failure model provides a mathematical relation between a root cause material and structural degradation to the change in subsystem and system level parameters. Simulating system behavior using these root cause degradation models provides a framework for predicting future system behavior.

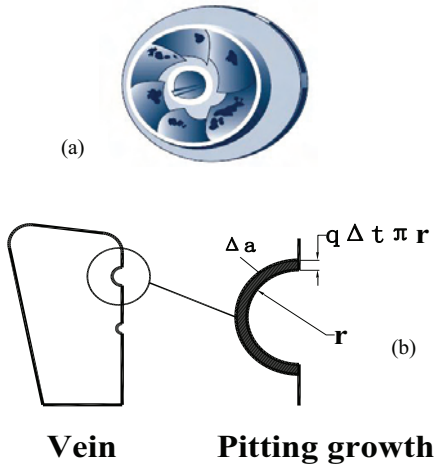


Fig. 5(a): Schematic corrosion/erosion damage to the vanes. (b) Schematic Pitting growth model

**Component Root Cause Model: Corrosion/erosion damage to vanes.** Fig. 5 illustrates how corrosion/erosion damage removes material from components, such as the pump rotor vanes. This reduces the total surface area of the vanes available for moving fluids. Also, the irregular surface of vanes may cause turbulence and reduce the efficiency in the fluid flow in the pump. The component model describes the loss in the cross-sectional area,  $a$ , of the vanes due to corrosion by detailed corrosion loss and local flow analysis. Making simplifying assumptions, the corrosion rate  $\dot{q}$  of the vane material is computed as  $\dot{q} = K(c_s - c_b)[2]$ , where  $K$  is the mass transfer coefficient dependent on the flow velocity,  $c_s$  is the corrosion product concentration at the liquid-solid interface dependent on the local temperature, and  $c_b$  is the concentration in the bulk flow and is often set to zero [2]. We assume constant flow velocity and temperature, and no change in fluid concentration. Thus,  $q$ ,  $K$  and  $c_s$  are constants. Further, we assume the corrosion damage to the vane occurs at its edge. The vane area loss is due the edge pitting growth. The growth pattern is assumed to be circular as shown in Fig. 5(b). The area loss at one pitting location can be expressed as

$$\Delta a_i = \dot{q} \pi r \Delta t = \dot{q} \pi r t \quad (4)$$

By integrating Eq. (4), we obtain the area loss at one pitting location as a quadratic function of time  $t$  (see Fig. 6). The total vane area loss  $\Delta a$  can be expressed as

$$\Delta a = \sum_{i=1}^n a_i = \frac{1}{2} \pi \kappa^2 t^2 \quad (5)$$

At a time instant  $t_j$ , the pump pressure and flow rate from Eq. (3) can be expressed as  $p_{out}^* = (a^* \theta - b \phi_{out}^*) \theta$ , where the superscript \* indicates the quantity is at the time instant  $t_j$ . Based on the first order perturbation theory, these quantities can be expressed as

$$\begin{cases} p_{out}^* = p_{out} + \Delta p \\ \phi_{out}^* = \phi_{out} - \Delta \phi \\ a^* = a - \Delta a \end{cases}$$

Combining Equations (4) and (5), and using the expression for  $p_{out}^*$  above, we get

$$p_{out} + \Delta p = a \cdot \theta^2 - \Delta a \cdot \theta - b \cdot \phi_{out} \cdot \theta + b \cdot \Delta \phi \cdot \theta.$$

Making further substitutions, and solving for  $\Delta a$ , we obtain  $\Delta a = \frac{b \Delta \phi \cdot \theta - \Delta p}{\theta^2}$ .  $\Delta a$ ,  $\Delta \phi$ , and  $\Delta p$  are all functions of  $t$  during

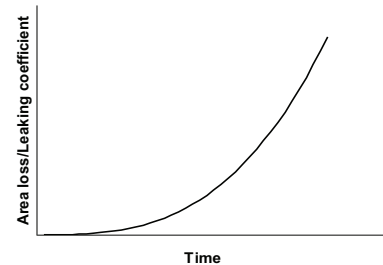


Fig. 6: Schematic plot of area loss function

the entire service life of the pump system. The resultant equation describing the time varying change of the cross sectional area of the vanes is given by

$$\Delta a(t) = \frac{b \Delta \phi(t) \theta - \Delta p(t)}{\theta^2}$$

This change propagated up to the subsystem pump model can be used to compute the change in pressure and outflow rate for the pump over time.

### Summary

This example and others, such as wear and fatigue damage to the seals, can be generalized to show that it is possible to detect the local damage by monitoring system level signals, such as angular velocities, fluid pressures, and fluid flow rates. The current examples represent simplified damage models. More detailed damage models need a more complex mechanical, fluid, and chemical analysis, which can enhance the understanding of underlying failure mechanisms attributed to structural and material damage.

### Deriving the Diagnosis Model

A number of different analytic modeling forms, such as state space, transfer function, and input-output model forms can be systematically derived from the topological HBG models [11],[14]. A particularly appealing topological model form that is derived from HBGs is the temporal causal graph (TCG), which forms the basis for our performance degradation analysis scheme. We have also derived efficient ways of deriving TCGs from HBGs [14].

TCGs capture causal and temporal relations among the system variables that characterize dynamic system behavior. They are an extended form of Signal Flow Graphs, with vertices representing the system variables (e.g., pressures, temperatures, and flow rates) and labeled directed edges capturing the relations between the variables. Labels on the edges further qualify the relations between the vertices. A label of  $\pm 1$  on an edge implies a direct (inverse) directional proportionality between the associated variables, and  $=$  implies an equality relation between the associated variables. Component parameters, R's, TF's, GY's, C's and I's appear on links, and play a role in establishing the relations between the associated variables. R, TF, and GY impose algebraic relations, whereas the energy-storage elements, C and I, impose integral, i.e., temporal delay relations between the associated variables. Fig. 7 shows the TCG derived from the BG model of the pump shown in Fig. 3.

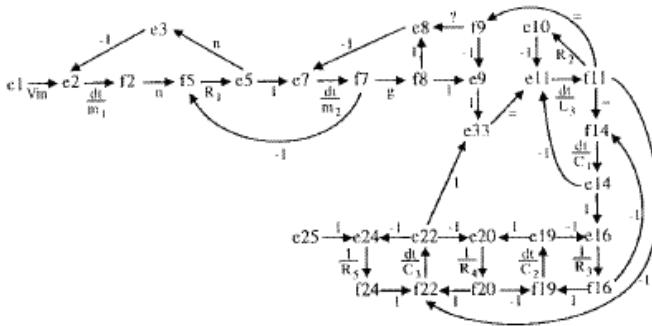


Fig. 7: Temporal Causal Graph of Secondary Sodium Cooling Loop

## Diagnosis and Prognosis Algorithms

Model-based methods for fault detection, isolation, and degradation use analytical redundancy methods. Discrepancies between observed and predicted measurement values are mapped back to constraints defined by the system model to isolate faults and degradations.

### Fault Detection, Isolation, and Identification (FDII)

Our FDII approach is innovative in that it combines efficient qualitative methods with quantitative parameter estimation techniques for on-line diagnostic analysis [3]. The core fault isolation scheme is designed for isolation of abrupt parameter value changes [15], but we have also extended this approach for analysis of incipient faults using Dynamic Bayes Nets.

The subsystem and system FDII analysis uses a numeric observer scheme implemented as an Extended Kalman filter [3] to track nominal system behavior, and statistical methods for fault detection that are robust to measurement noise and small modeling errors [11]. Fault detection triggers a symbol generator, which codes measurement deviations as symbolic deviations in signal *magnitude* ( $+ \rightarrow$  above normal, and  $- \rightarrow$  below normal) and *slope* ( $+ \rightarrow$  increasing,  $0 \rightarrow$  flat, and  $- \rightarrow$  decreasing). The observed deviations are compared against symbolic fault signatures derived from the TCG to hypothesize parameter value changes that are consistent with the measurements. As additional measurements deviate, the isolation algorithm prunes the fault candidates to a small number of possibilities [14] [15]. Fault identification uses search methods to perform quantitative parameter estimation on the reduced candidate set using least square error techniques [3].

In our modeling framework, faults and degradations are expressed as changes in component parameter values. For example, a degradation in the pump performance could be linked to parameters like the transformer coefficient,  $n$ , rotor cross sectional area,  $a$  (chipping of the rotor vanes) or friction parameter,  $R_1$ . Faults and degradations are characterized by a parameter name and a direction of change. A decrease in pump efficiency is represented as  $n^-$ , an increase in the friction is captured as  $R_1^+$ , and decrease in rotor vane cross sectional area is modeled as  $a^-$ . For pipe 2,  $R_2^+$  implies a partial block whereas  $R_2^-$  implies a leak in the pipe.

Simulation studies conducted on the system demonstrated the effectiveness of the FDI approach. The seven measured variables in the secondary sodium loop system are  $f_2$  and  $f_7$  – the inflow rate and outflow rates at the pump,  $e_{33}$  – fluid pressure at the pump,  $e_{14}$ ,  $e_{19}$ , and  $e_{22}$  – the fluid pressures at the super heater, evaporator and overflow tank, respectively. The measurement sampling rate was chosen as 1 sec., and faults were introduced in the system by changing the parameter values (in most cases the parameter value was doubled or made half) at a specific time point. Measurement noise was set at 2%. The fault isolation results for a representative set of faults are summarized in

Table 1. In some cases the qualitative FDI algorithm could not generate a unique fault candidate, but the actual single fault was always included as part of the diagnosis result. The last column presents the average time to diagnosis over five runs. The time to isolation varies from experiment to experiment because of the noise in the measured signals. As the signal to noise ratio decreases the time to detection and isolation also increase [13].

**Table 1: Fault Isolation results assuming 2% noise in the measured signal**

Number	Fault	Diagnosis Result	Time to Isolation (seconds)
1	$R_1^+$	$(n, R_1^+)$	58
2	$R_2^+$	$R_2^+$	27
3	$R_2^-$	$R_2^-$	46
4	$R_3^+$	$R_3^+$	125
5	$R_3^-$	$R_3^-$	699
6	$R_4^+$	$(R_4^+, R_5^+)$	378
7	$R_4^-$	$(R_4^-, R_5^-)$	43
8	$C_{SH}^-$	$C_{SH}^-$	16
9	$C_{EV}^-$	$C_{EV}^-$	45
10	$C_{OFC}^-$	$C_{OFC}^-$	9
11	$m_2^-$	$m_2^-$	5
12	$I_{HX}^-$	$I_{HX}^-$	11

Following isolation at the system level, the diagnosis scheme invokes the more detailed component-level algorithm to establish the root cause for the identified faulty component parameter. For example, initial system level fault isolation may point to a change in pump parameter,  $a$ , the rotor cross sectional area. Further analysis of the pump behavior using the relevant pressure and flow measurements may yield pitting growth in the rotor veins attributed to corrosion damage as the root cause for decrease in pump efficiency. Having established the material and structural causes for the discrepancy or fault to the subsystem parameter change, in this case the curvature of the rotor vein,  $a$ , we derive the temporal profile for the parameter value change. This forms the basis for running simulation-based prognosis algorithms that predict future system behavior and performance.

### Prognosis by Simulation

Our model-based prognosis scheme implements three interconnected modules: (i) a POF-based simulator for predicting future system behavior, (ii) mechanism to compute performance measures that are relevant to determining system health and safety, and (iii) a decision scheme embedded in the supervisory controller that uses the performance measures to make decisions on reconfiguration and continued operation versus scheduling downtime and maintenance.

**The Simulation Scheme.** Our simulation models for prognosis capture the temporal profiles (i.e., the rate of change of parameter values) of faults and degradations, and use this information to generate accurate predictions of future system behavior from the current state taking into account different operating modes of the system. The prognosis

computations include multiple sources of uncertainty in the models, in the system measurements, and in the modes of system operation. The prognosis scheme combines adaptive top-down and bottom-up procedures: (1) the basic forward prediction using Monte Carlo simulations combines the effects of different sources of uncertainty and quantifies the overall uncertainty in the prognosis prediction; (2) the simulation also helps identify the dominant sources of the uncertainty, and this is followed up by additional data collection and refinement of modeling efforts to reduce some of the uncertainties; and, (3) the forward prediction computations are updated by re-running the simulation from the current state with the new information. The prognosis step may be repeated multiple times to make the future behavior predictions more accurate. The Bayes net methodology is particularly beneficial in implementing this scheme [9]. When new information is obtained for one of the network nodes, the information is propagated to all other nodes in the network. In addition to providing a mechanism for refining the component mathematical models this approach provides a framework for extrapolating our prognosis and prediction methods from laboratory to field conditions and nominal to extreme conditions [10],[16].

The prognosis task is further complicated by the fact that the environment and mode of system operation in the future are unknown, and have to be derived from past operations and knowledge of system behavior. We contend that data for modeling, diagnosis, and predictive behavior analysis will have to come from three different sources: design, mission, and maintenance. The design data will aid bottom-up analysis, while mission and maintenance data will facilitate top-down fault detection first, and then propagate through the bottom-up analysis for system health and capability assessment. Mission data will help define and validate the models of the dynamic behavior of the system for different operating conditions, and maintenance data will be directly linked to parameters of the physics of failure models for root-cause analysis. Thus tailoring the diagnosis and prognosis methods to the available data is a crucial step in ensuring the feasibility of our proposed methodology.

Simulating complex models is fairly resource intensive, and the ability to customize the system models based on needs is critical. Our modeling approach, discussed earlier allows for the construction of simulation models on the fly with appropriate physical system model refinement to balance model precision and simulation accuracy. It should be clear that the simulation models include the system controllers, and the control strategies are allowed to adapt during the simulation, just like the real system.

**Uncertainty Analysis.** Uncertainties in approximate, reduced-order material life and component models need to be validated by sensitivity analysis and analytical simulation methods, and stochastic finite element and stochastic response surface methods. These methods also help to quantify uncertainty propagation from one level of data analysis to the next (signal processing vs. feature extraction) or one level of modeling to the next (microstructure vs. macros-

copic). Life prediction models range over wide scales, such as structural level (i.e., secondary sodium loop system), component level (i.e., the rotor, bearings, and seals in the pumps), coupon level (i.e. small specimen tests) and micro-structural level (i.e. grain and sub-grain fatigue crack analysis). Using analytical techniques, uncertainties within the micro structural level (e.g., grain size and shape, slip plane orientations, initial defects) can be used to simulate the randomness of fatigue properties at the material and component level. Computational effort in multi-level uncertainty propagation analysis can be reduced through efficient techniques such as multi-resolution finite element analysis, design of experiments, and adaptive sampling [8], [17].

Uncertainties are present in all phases of damage prognosis of components, including those caused by natural variability, measurement errors, modeling errors, parameter assumptions, solution approximations, etc. These uncertainties are usually classified into two categories: (1) aleatoric uncertainty, i.e., inherent or natural variability, and (2) epistemic uncertainty which occurs due to lack of knowledge. If the variance in a particular parameter is found to significantly affect the prognosis result, then more data collection resources should be allocated to reduce the data uncertainty in that parameter. In the case of epistemic uncertainty, which is caused by lack of knowledge, various approaches such as additional data collection, improved analytical modeling of the physics, incorporation of expert opinion, Bayesian updating, model calibration, etc., can be used to reduce the uncertainty. A systematic prognosis architecture needs to be developed that properly quantifies and incorporates the effects of various types of uncertainties at various levels, and that includes a top-down optimization approach that effectively allocates resources for uncertainty reduction.

### **Prognosis, Decision Making, and Control**

In work we have done thus far, prognosis is looked upon as a combination of prediction with an assumed POF degradation model that is evaluated in the context of a realistic resource management strategy [1]. Therefore, our measures compute the predicted use of resources (e.g., power consumption and water consumption). Other metrics specify thresholds on system variables and parameters, and can be linked to system safety (e.g., pressure in a pipe should be kept less than  $p_0$ , otherwise the pipe is likely to burst).

Decision making schemes use the predicted measures to compute when performance and resource levels may decrease below predefined values that are determined by safety and reliability concerns. The safety measures with implied thresholds also indicate when to terminate system operation and go into maintenance mode. The decision making scheme, is built into the supervisory control scheme, and includes maintenance and reconfiguration options (currently these are coded as rules).

The objective of system health and capability assessment is to facilitate decision-making such as in-flight actions, maintenance scheduling, logistics management, etc. How-

ever, these decisions have to be made under various types of uncertainty (such as, sensor performance, measurement errors, modeling errors, parameter variability, operating conditions, future demands). Thus decision-making under uncertainty needs to maximize the performance under several risk, cost, and schedule constraints.

## **DISCUSSION AND CONCLUSIONS**

The modeling, monitoring, and FDI approaches discussed above as part of the performance monitoring framework have been applied to a number of complex systems, such as the secondary sodium cooling loop of a nuclear reactor [14], the cooling systems of automobile engines [5], fuel transfer systems of fighter aircraft [15], and Advanced Life Support Systems for long duration NASA missions [4]. All of these systems are multi-domain. For example, the secondary sodium cooling loop has subsystems that encompass the electrical, mechanical, and fluid domains, and the system primarily modeled energy exchange between the fluid and thermal domains. The cooling system of the automobile engines and the ALS systems were based on similar modeling paradigms. Also, all of the systems include highly nonlinear and hybrid behaviors. The diagnosers developed combined qualitative reasoners based on TCGs with quantitative parameter estimation methods. In other work, we have extended our diagnosis schemes to perform fault-adaptive control and resource monitoring [1]. These approaches are the first steps toward comprehensive performance monitoring of vehicular systems.

This paper has discussed an integrated architecture for ISHM that combines diagnosis, fault-adaptive control, and prognosis. A common component-oriented modeling framework provides the core around which the different analysis schemes are designed. Furthermore, ISHM is looked upon as a key component of a control architecture to support the safe and efficient operation of complex systems. The control architecture, described as a three-level scheme, connects the real-time temporal scale for robust control, to a short-time horizon performance-based fault-adaptive control scheme at the intermediate level, to a longer time horizon performance and resource-based supervisory control scheme at the highest level. The role of monitoring, diagnosis, and simulation-based prognosis in supporting this control architecture has also been discussed. We have presented the algorithms we have developed for supporting this ISHM architecture. This approach has been successfully applied to managing components of an Advanced Life Support system (ALSS) for a simulated 90 day manned mission to a lunar habitat.

In future work, the simulation-based prognosis scheme and the decision-making schemes of the supervisory controller will be extended with more sophisticated probabilistic reasoning and decision analysis schemes. We will develop systematic decision theoretic schemes that can handle situations like a subsystem shutdown followed by an estimated repair time, and startup. This will support the

analysis of trade-offs between the utility of maintenance versus continued operation in degraded mode.

## REFERENCES

- [1] Abdelwahed, S., Wu, J., Biswas, G., Ramirez, J., and Manders, E.J., "Online adaptive control for effective resource management in advanced life support systems," *Habitation - An International Journal for Human Support Research*, vol. 11, no. 2, pp. 105–115, Feb. 2005.
- [2] Balbaud-Celerier, F. and F. Barbier, *Journal of Nuclear Materials*, 289, 227, 2001.
- [3] Biswas, G., Simon, G., Mahadevan, N., Narasimhan, S., Ramirez, J., and Karsai, G., "A robust method for hybrid diagnosis of complex systems", *Proc. 5th IFAC Symposium on Fault Detection Supervision Safety Technical Processes*, pp. 1125–1131, Washington, DC, June 2003.
- [4] Biswas, G., Manders, E.J., Ramirez, J., Mahadevan, N., and Abdelwahed, S., "Online model-based diagnosis to support autonomous operation of an advanced life support system," *Habitation: An International Journal for Human Support Research*, vol. 10, no. 1, pp. 21–38, Jan. 2004.
- [5] Feenstra P.J., et al., "Bond Graph Modeling Procedures for Fault Detection and Isolation of Complex Flow Processes", in *Proc. ICBGM'01*, Edited by Jose J. Granda and Genevieve Dauphin-Tanguy, Simulation Series, vol. 33, no. 1, SCS Publication, ISBN 1-56555-221-0.
- [6] Jaw, L.C. and R. Friend. "ICEMS: A platform for advanced condition-based health management," *Proceedings of the Aerospace Conference*, 2001.
- [7] Karnopp, D.C., Margolis, D.L., and Rosenberg, R.C., *System Dynamics: Modeling and Simulation of Mechatronic Systems*, Wiley Interscience, NY, NY, 1999.
- [8] Liu Y., and Mahadevan S., "Multiaxial High-Cycle Fatigue Criterion and Life Prediction for Metals", *International Journal of Fatigue*, vol. 7, Issue 7, pp. 790-800, 2005.
- [9] Mahadevan, S., Zhang, R., and Smith, N., "Bayesian networks for system reliability reassessment," *Structural Safety*, pp. 231-251, 2001.
- [10] Mahadevan, S. and Rebba, R., "Validation of reliability computational models using Bayes networks." *Reliability Engineering and System Safety*, **87**(2), 223–232, 2005.
- [11] Manders, E.J., Biswas, G., Ramirez, J., Mahadevan, N., Wu J., and Abdelwahed, S., "A Model Integrated Computing Tool-Suite for Fault-Adaptive Control," *Proc. 15th Annual Workshop on Principles of Diagnosis*, L. Trave-Massuyes, ed., Carcassonne, France, pp. 137-142, June 2004.
- [12] Mosterman, P.J., "Hybrid dynamic systems: A hybrid bond graph modeling paradigm and its application in diagnosis," *Ph.D. dissertation*, Vanderbilt Univ., Nashville, TN, 1997.
- [13] Mosterman, P.J. and G. Biswas, "A theory of discontinuities in physical system models," *Journal of the Franklin Institute*, vol. 335B(3), pp. 401–439, 1998.
- [14] Mosterman, P.J. and Biswas, G., 'Diagnosis of continuous valued systems in transient operating regions', *IEEE Trans. Systems, Man, and Cybernetics, Part A*, vol. 29, no. 6, pp. 554–565, 1999.
- [15] Narasimhan, S. and Biswas, G., "Model-based Diagnosis of Hybrid Systems," *IEEE Trans. on Systems, Man, and Cybernetics, Part A*, to appear, 2007.
- [16] Rebba, R., and S. Mahadevan, "Validation and Error Estimation of Computational Models," *Reliability Engineering and System Safety*, 2005.
- [17] Zou, T., Mahadevan, S., Mourelatos, Z., and Meernik, P., "Reliability Analysis of Automotive Body-Door Subsystem," *Reliability Engineering and System Safety*, Vol. 78, No. 3, pp. 315-324, 2002.